ARTICLE NO. 79-0666R

Airframe Noise Measurements on a Supersonic Transport Small-Scale Model

John S. Preisser*
NASA Langley Research Center, Hampton, Va.

Airframe noise has been measured on a 0.015 scale model of an advanced supersonic transport concept (AST-100) in an anechoic flow facility. The model was equipped with leading- and trailing-edge flaps, nose and main landing gears, and engine nacelles. Each of these components was deployed, individually and collectively, to determine their contribution to the noise field. Results are presented which show that in the clean configuration the aircraft displays a symmetric dipole directivity, whereas in the more complex landing-approach configuration the directivity peaks in the forward quadrant. It was found that the landing-approach noise was due chiefly to the landing gear, the trailing-edge flaps, and the aeroacoustic interaction between the two.

Introduction

SEVERAL years ago, airframe noise was recognized as a lower limit to the reduction of noise levels that could be achieved by further decreases in propulsion noise of commercial aircraft.[1] At that time, indications were that airframe noise produced by a large subsonic aircraft during landing-approach lay only about 10 EPNdB below the FAR-36 certification levels. This result promoted research aimed at understanding and controlling the causes of airframe noise and predicting the levels. Flyover noise measurements were performed by various investigators on configurations which varied from gliders to large transport jets at reduced power settings. (A fairly complete recent listing of those aircraft used since 1970 specifically for airframe noise studies may be found in Ref. 2.) Semiempirical prediction schemes were developed, and subsequently updated as the experimental data base grew. Presently, overall sound pressure levels can be predicted reasonably well based upon simple analytic expressions which involve only velocity, wing area, and source-observer distance. Spectra and directivity can also be predicted fairly well for conventional aircraft given the geometric definition of the landing gear and flap system.[3] Some uncertainty remains, however, about how well the prediction schemes will apply to the nonconventional, advanced configurations of the future.

Paralleling the development of airframe noise understanding and prediction has been renewed interest by both industry and NASA in conducting technology assessment studies on supersonic cruise aircraft. The NASA Supersonic Cruise Aircraft Research (SCAR) program was created with the goal of identifying key technologies that would require further study to improve aerodynamic efficiency, reduce operating costs, and provide environmentally acceptable noise and pollution emissions for future supersonic transport aircraft. As part of the noise assessment, airframe noise was considered since it posed a potential lower limit to any reduced certification levels that could be enacted. Presently, the FAA's goal is not to certify, or to permit to operate in the United States, any future design SST that does not meet standards then applicable to subsonic airplanes.

This paper presents results from airframe noise tests on a small-scale model of a supersonic transport concept in an anechoic flow facility. Very little data exist on complete aircraft models in such flow facilities. Tests on a large transport model have been reported[4] and encouraging results in regard to scaling were obtained. The present model was a 0.015 scale AST-100. The AST-100 was an earlier configuration considered in the SCAR program which had undergone extensive aerodynamic testing at several model scales. Low-speed aerodynamic characteristics of this configuration have been investigated using both a 0.10 scale model[5] and a 0.015 scale model. Unpublished data from the latter model indicated the overall aerodynamic performance trends were not affected by scaling down to the smaller model size. Nevertheless, a force balance was included in the present model tests to insure compatibility with the published aerodynamic results.

The tests were conducted at the NASA Langley Aircraft Noise Reduction Laboratory in the Anechoic Flow Facility. Previous exploratory tests[6] using a similar model showed that useful data several decibels above the facility background noise could be achieved. The purpose of the present test was to determine quantitatively at model scale the airframe noise levels and to identify the airframe components which contribute significantly to those levels. The model was equipped with leading- and trailing-edge flaps, nose and main landing gear, and engine nacelles. Each of the components was deployed, individually and collectively, to determine their contribution to the noise field. Acoustic data are presented which include one-third octave band spectra and directivity in both the flyover and sideline planes for various configurations. Effects of flap deflection and aircraft angle of attack are also presented. The use of model data for assessing full-scale levels is discussed.

Description of Model and Experimental Method

Model

The test model was a 0.015 scale AST-100. Details of the full-scale geometry may be found in Ref. 5. Pertinent dimensions of the model geometry are presented in Table 1. The model was of lightweight fiberglass construction and had an overall length of 1.40 m and a wing span of 0.61 m. Photographs of the model showing the component construction are presented in Fig. 1. Figure 1a shows the topside of the model and its flap system; Fig. 1b shows the model underside and the engine nacelles and landing gear. The large, leading-edge flap near the forward section of the fuselage (hereafter referred to as the apex flap) was equipped with two sets of brackets for testing at 0 and 30 deg deflection. Two sets of wing tips allowed testing at two different leading-edge/trailing-edge combinations, namely 0/0 and 45/5 deg.

Presented as Paper 79-0666 at the AIAA 5th Aeroacoustics Conference, Seattle, Wash., March 12-14, 1979; submitted April 2, 1979; revision received March 21, 1980. This paper is declared a work of the U.S. Government and therefore is in the public domain.

Index categories: Noise; Aeroacoustics.

*Aerospace Engineer, Acoustics and Noise Reduction Division. Member AIAA.

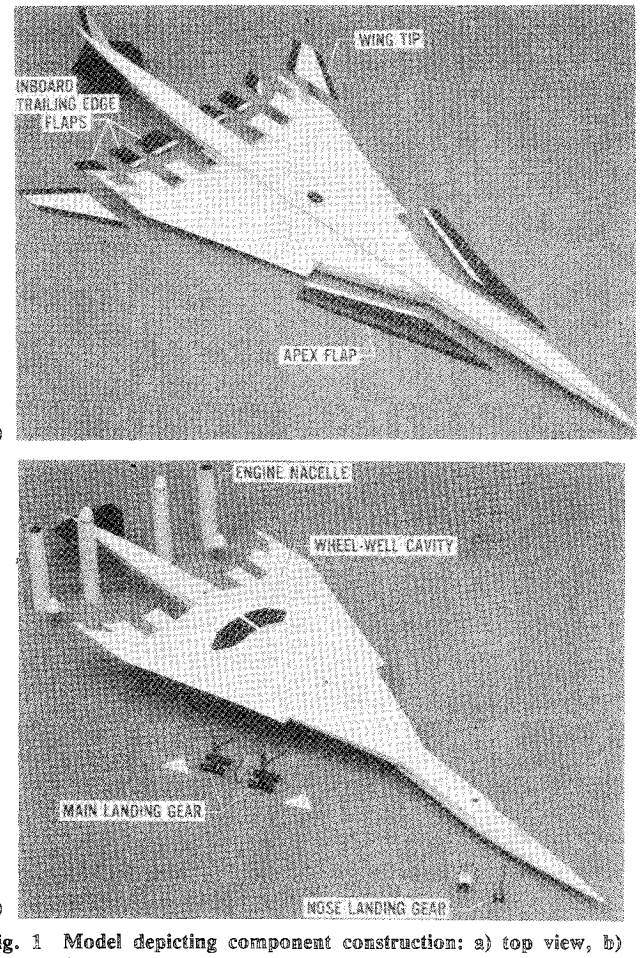

Fig. 1 Model depicting component construction: a) top view, b) bottom view.

Table 1 Model geometry

Wing area, S, m^2	0.23
Span, b, m	0.61
Aspect ratio, AR	1.72
MAC, $\bar{c}$, m	0.51
Root chord, m	0.84
Tip chord, m	0.08
Thickness, t/c, % (approximately)	3
Leading edge sweep, deg	
Inboard	74
Midspan	70
Outboard	60

The inboard trailing-edge flaps (three on each semispan) had five sets of brackets preset in 10 deg increments covering a flap deflection range of 0 to 40 deg. All flap brackets were full span, flush-mounted, and allowed no gaps or slots when mounted. The hole in the top of the fuselage seen in Fig. la provided access for the force balance to be affixed to the model center of gravity. The model was equipped with four engine nacelles which were mounted on the underside of the wing. These nacelles could be tested in a flow-through mode or with either the front end or both ends plugged. The main landing gear consisted of two sets of 12-wheel assemblies attached to a rigid strut with side brace. Each gear extended up into shallow wheel-well cavities. Simulated doors hung from either side of each cavity when the landing gear was deployed. The nose gear consisted of a two-wheel assembly attached to a simple strut with simulated doors which also extended up into a shallow cavity. A transition strip of fine sand was applied to the leading 5% chord across the full span in order to insure a turbulent boundary layer representative of high Reynolds number conditions. The landing gear was also treated with sand to inhibit laminar vortex shedding.

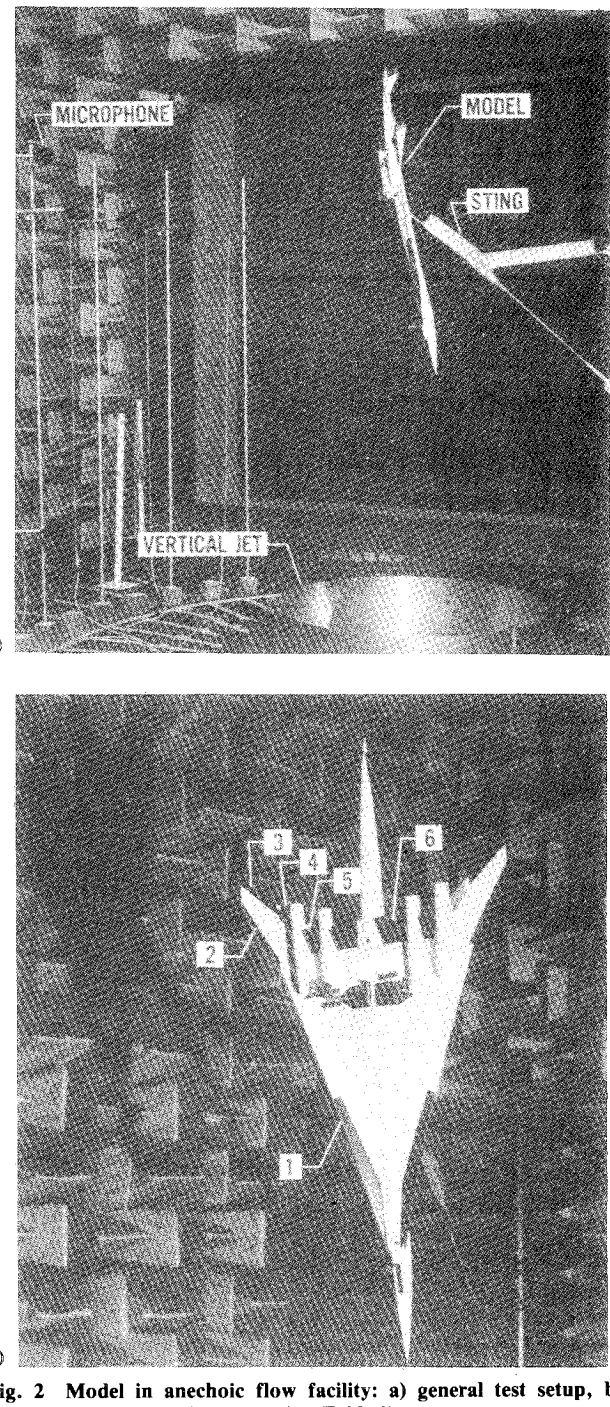

Fig. 2 Model in anechoic flow facility: a) general test setup, b) landing-approach configuration (see Table 2).

Test Setup and Procedure

Figure 2 shows photographs of the model mounted in the anechoic room. The general test setup is indicated in Fig. 2a and a close-up of the model in the landing-approach configuration is shown in Fig. 2b. The room was $6.1 \times 9.1 \times 12.2$ m high and had 0.84 m deep fiberglass acoustical wedges on the walls and ceilings. Portable wedges were placed over the metal floor grating prior to acoustic testing. The model was sting-mounted through the top side and positioned in a nose-down attitude. The sting entered the model at a height of approximately 1.83 m above the jet exit and provided the capability for angle-of-attack change. Airflow was provided by a 1.22 m diameter vertical jet nozzle, which was driven by a centrifugal fan that was housed in another building to minimize extraneous background noise from entering the facility. Tests were run over an angle-of-attack range of 0 to 20 deg at velocities between 18 and 34 m/s.

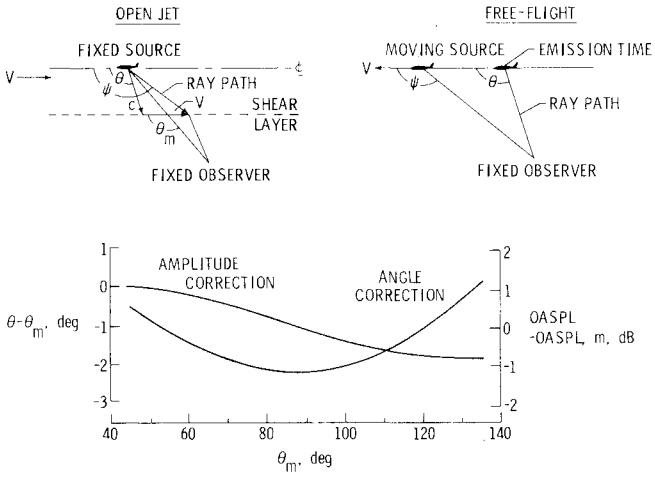

Fig. 3 Shear layer corrections, $V = 30$ m/s.

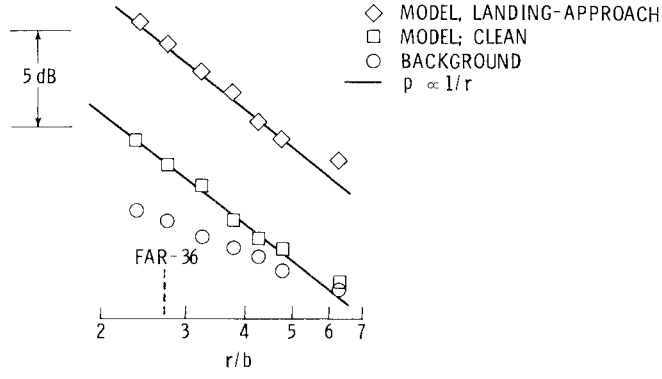

Fig. 4 Change in overall sound pressure level with radial distance from jet centerline.

Table 2 Flap settings for typical landing-approach configuration

Position	Number (see Fig. 2b)	Setting
Apex	1	30 deg
Leading edge (tip)	2	45 deg
Trailing edge (tip)	3	5 deg
Trailing edge	4	40 deg
Trailing edge	5	40 deg
Trailing edge	6	40 deg

Instrumentation

Both acoustic and aerodynamic parameters were measured. Acoustic data were taken with six 0.5 in. condenser-type microphones: four were mounted on poles at a height corresponding to the model-to-sting attachment point, the remaining two were mounted in tandem on a vertical traversing mechanism. The former were used to measure sideline directivity, the latter provided directivity data in the flyover plane. The microphones were placed about 1.7 m from the model. This position corresponded to the appropriately scaled FAR-36 measuring point for approach (that is, the ratio of source-observer distance to wing span $r/b = 2.7$ is the same as it would be for a full-scale aircraft on a 3 deg glide slope at 1 n. mi. from the threshold).

All acoustic data were high-pass filtered at 200 Hz, amplified, and recorded on magnetic tape at 30 in./s for post-test data analysis.

Outputs of two orthogonal axes of the strain gage-type force balance were taken online and resolved to yield lift and drag by an angular transformation. The data were corrected for balance interaction effects but were not corrected for jet boundary effects.

Test Environment

Flowfield

Both pitot tube and hot-wire surveys were made at several heights above the jet exit plane. It was desired to position the model high enough to minimize acoustic reflections from the jet nozzle, but low enough to keep the wing tips out of the turbulent jet shear layer. It was found that the jet spread much like a classical subsonic jet with the potential core extending approximately six nozzle diameters downstream. Both mean and turbulent velocity profile shapes were independent of velocity and the mean flow was uniform within 1 to 2%. The model was placed in a position where the potential core was about 0.94 m wide having turbulence levels on the order of 0.5%. This was determined to be sufficient for the aircraft to be in uniform low turbulent flow simulating conditions encountered during flight through the atmosphere.

Shear-Layer Corrections

Testing in an anechoic flow facility provides a different acoustic situation than the actual aircraft flyover which one attempts to simulate. The differences are indicated on the top of Fig. 3. In the open jet situation, both the source and observer are in fixed positions. An acoustic ray emanating from the source is convected downstream until it encounters the jet shear layer where it becomes refracted back upstream. In the free-flight situation, the source is moving while the observer is fixed. While an emitted ray travels toward the observer, the aircraft is moving and is at some new position when the ray reaches the observer. The measured airframe noise data θ_m in this paper have been converted to the source emission angle θ using a theoretical method[7] which models the shear layer as an infinitely thin vortex sheet. At a free jet flow of 30 m/s, the corrections for both amplitude and direction were small and are shown at the bottom of Fig. 3.

Results and Discussion

In this part of the paper, results are presented and discussed for the clean airframe, the individual airframe components, and the landing-approach configuration. The question of scaling the model data to full-scale is also addressed.

The change in overall sound pressure level with radial distance from the jet centerline for the free jet with sting (background), the clean configuration, and the landing-approach configuration is presented in Fig. 4. Radial distance r has been normalized to the wing span b. The clean configuration corresponds to all flaps set at 0 deg deflection, with all landing gear removed and associated wheel-well cavities plugged to provide a smooth lower wing surface contour. The landing-approach configuration has the landing gear deployed and flaps deflected at those values given in Table 2. In this figure (and for all the data shown in this paper), the background noise has been subtracted from the model data. For the closest radial distance, the model in the clean configuration is about 4 dB above the background, while the landing-approach noise is about 10 dB above. At the farthest radial distance, the differences are much less. For reference, the change of sound pressure level for a compact source in a free field environment ($p\alpha 1/r$) is also shown. The good agreement between the data and the reference would suggest that even though the model is large, the noise source regions are most likely localized to a small area. Also, for reference, the scaled FAR-36 measuring point for approach is indicated. Most of the data in this paper will correspond to the FAR-36 condition, since this position yielded a good signal-to-background noise ratio and eliminated the need for geometric considerations when scaling the model data to full-scale results.

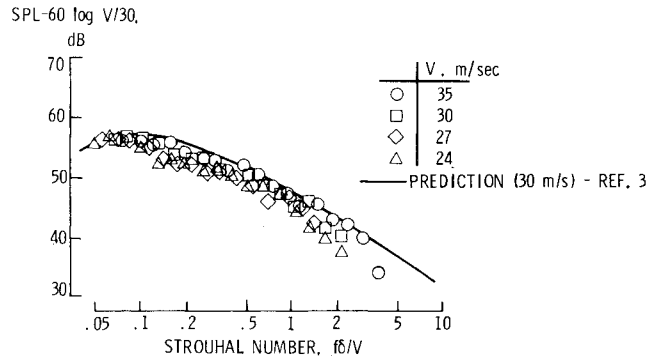

Fig. 5 Normalized one-third octave band spectra for clean configuration, $\theta = 90$ deg, $\phi = 0$ deg.

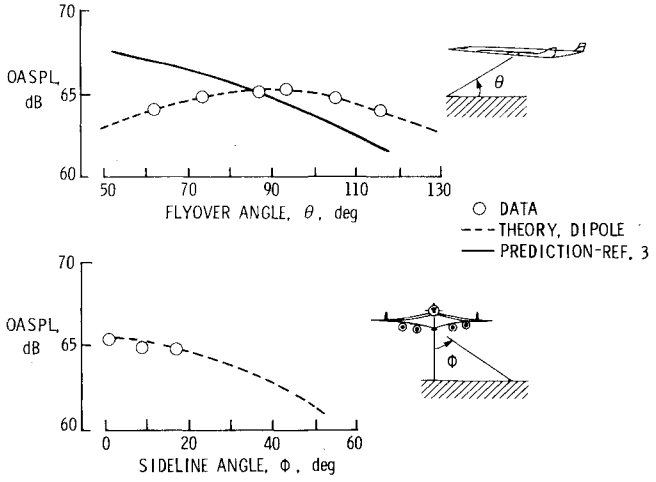

Fig. 6 Directivity pattern for clean configuration, $V = 30$ m/s.

Clean Airframe

Spectra

Normalized one-third octave band spectra for the clean airframe at an angle of attack of 8 deg are presented in Fig. 5. The sound pressure level has been normalized by 60 log $V/30$, where V is the jet velocity. The frequency has been nondimensionalized by δ/V, where δ is the boundary-layer thickness at the trailing edge of the wing. Following Ref. 3, this thickness was calculated as one for a flat-plate turbulent boundary layer that had developed over a distance corresponding to the mean aerodynamic chord. It is seen that the data collapsed reasonably well using these parameters. Also, the data are seen to agree on a quantitative basis with the prediction of Ref. 3. This agreement suggests that the clean model data will scale, since the prediction method is semiempirical and based upon full-scale flyover data of various aircraft. However, Ref. 3 assumes a V^5 velocity dependence on the noise while the present study shows a V^6 dependence. The V^5 dependence has as a theoretical basis[8] the scattering of turbulent eddies near the edge of a semi-infinite plane. The semi-infinite plane would be a good approximation to the present case only for sufficiently high frequencies. The present data are dominated by low frequencies, and peaks at a wavelength whose size is on the order of the mean aerodynamic chord. Hence, a different mechanism may be responsible for the noise production.

Directivity

The directivity of the clean airframe in both the flyover and sideline planes is presented in Fig. 6. The data were corrected using the information contained in Fig. 3 and adjusted to constant radius from the source. Excellent agreement is obtained between the data and a theoretical representation of the noise source as a dipole. The dipole representation has a $\sin^2\theta$ dependence for the mean-square pressure. In contrast, the Ref. 3 prediction employs a $\cos^2(\theta/2)$ dependence which overpredicts in the forward arc and underpredicts in the aft direction. The reason for the difference in directivity between the present data and Ref. 3 is unknown. However, the data base of Ref. 3 contains chiefly conventional aircraft, while the AST-100 incorporates a low-aspect-ratio arrow wing characterized by large leading-edge sweep (see Table 1). At moderate-to-high angles of attack ($\alpha > 6$ deg) local regions of vortex separation occur along the leading edge.[9] This vortex system (which dominates the aerodynamic behavior of the configuration) may also dominate the aeroacoustic scene, resulting in a whole body lift dipole.

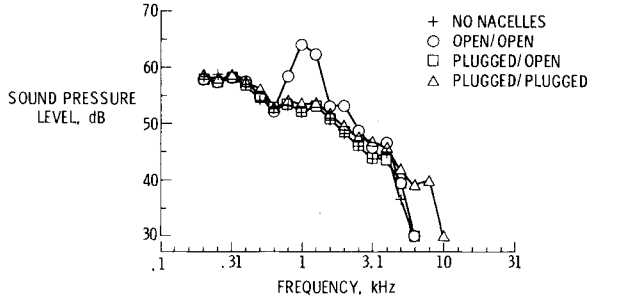

Fig. 7 Effect of engine nacelles on one-third octave band spectra, $V = 30$ m/s, $\theta = 90$ deg, $\phi = 0$ deg.

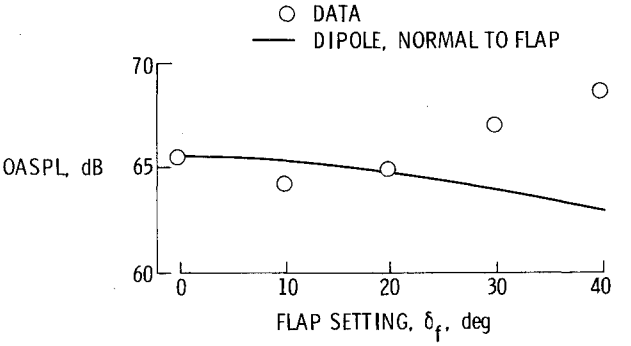

Fig. 8 Variation of overall sound pressure level with trailing-edge flap setting, $V = 30$ m/s, $\theta = 90$ deg, $\phi = 0$ deg.

Component Noise Levels

Each of the major model components was tested individually on the clean airframe in order to identify the noise radiation from each item independent of the other noise sources. It was found that the trailing-edge flaps, the main landing gear, and one particular nacelle configuration had significant (>0.5 dB) contributions above the clean aircraft level. The apex flaps, the leading-edge/trailing-edge wing-tip combination, and the nose gear made little if any contribution to the noise field.

Effects of Nacelles

The AST-100 configuration has four engines mounted on the underside of the wing and extending slightly past the wing trailing edge (refer to Fig. 2b). The nacelles were modeled in the present tests with 2.5 cm diameter brass tubing that had an overall length of 17.2 cm. A short pylon was used to fit each cylindrical nacelle to the contoured lower wing surface. The nacelles were provided with both front- and aft-end plugs having the shape of a paraboloid. It was uncertain a priori as to the best method of modeling the flowfield about and through a nacelle, so tests were performed to determine the sensitivity of several configurations to the acoustic radiation. Results are shown in Fig. 7. There is little if any difference

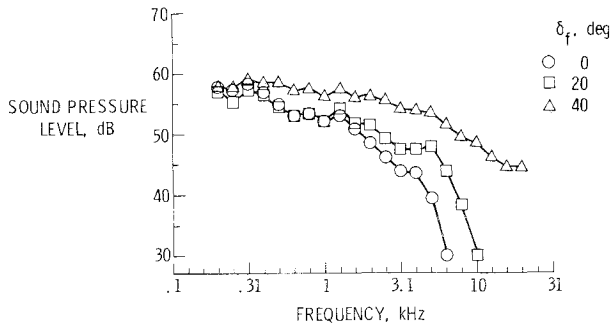

Fig. 9 Variation of one-third octave band spectra with trailing-edge flap setting, $V=30$ m/s, $\theta=90$ deg, $\phi=0$ deg.

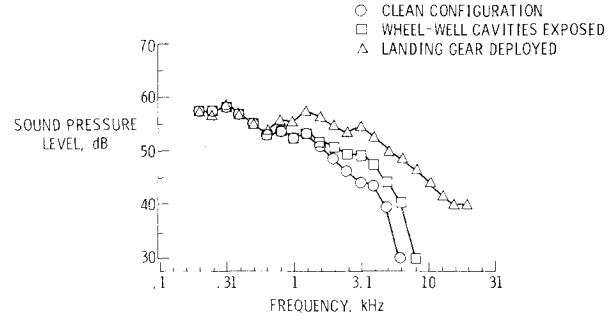

Fig. 10 Effect of main landing gear on one-third octave band spectra, $V=30$ m/s, $\theta=90$ deg, $\phi=0$ deg.

between the airframe with nacelles removed and the two configurations with the front ends plugged (plugged/open and plugged/plugged). The unplugged (flow-through) configuration provided a 10 dB noise increase in a narrow frequency range around 1000 Hz. This acoustic radiation corresponds to the fundamental resonance frequency of a pipe with two open ends. Since such a standing wave pattern could not exist internal to a real jet engine, it was concluded that the flow-through configuration was unrealistic and engine nacelles, in general, make a negligible contribution to airframe noise. The remaining tests involving nacelles were performed using a front-end plug.

Effects of Flap Deflection

Overall sound pressure level as a function of flap deflection angle is presented in Fig. 8. All six inboard trailing-edge flaps had the same setting. The data correspond to the $\theta=90$ deg, $\phi=0$ deg overhead position. It is generally accepted by most investigators[2,3] that flap noise is caused by the convection of wing-generated turbulence past the flaps producing lift force fluctuations. This results in a dipole radiation pattern which peaks in a direction normal to the flaps. If the noise source strength does not change with flap deflection, then for a fixed observer position beneath the aircraft the noise level would decrease with increasing flap deflection (due solely to rotation of the dipole axis). This is indicated by the solid line on the figure. Note that the data show an increase in level for the higher deflection angles. This implies an increased noise source strength. Published aerodynamic data[5] on the AST-100 indicate that flow separation occurs on the upper surface at the 30 and 40 deg flap settings. It is believed that the highly turbulent separated flow convecting past the flap trailing edge would contribute to the increased noise source strength as observed in the figure.

In Fig. 9 is presented one-third octave band spectra for several flap deflection angles. Increasing flap deflection causes increased high-frequency noise radiation. The largest increase is for $\delta_f=40$ deg, which is consistent with the previous figure.

Table 3 Component noise contributions

OASPL - OASPL (CLEAN), dB			
	$\theta=60$ deg	90 deg	120 deg
Apex flap	*	*	*
Leading edge flaps	*	*	*
Trailing edge flaps	3.6	2.8	1.4
Nacelles	*	*	*
Nose gear	*	*	*
Main gear	2.0	2.1	2.1
Σ components	4.6	4.0	3.0
Landing-approach configuration	7.2	5.2	3.6

* Less than 0.5 dB.

Effects of Landing Gear

Landing-gear noise is composed of sound generated by the interaction of flow with the wheel-well volume and the external landing gear.[10] Depending upon geometry and Reynolds number, isolated wheel-well related sound can be characterized by both broadband noise and discrete tones whose intensity is reduced by the spoiling effect of the gear. Also, externally generated landing-gear noise can either be discrete or have broadband character. In the present tests the nose landing gear had no measurable effect on airframe noise. The main landing gear was found to have a large effect. In Fig. 10 are presented noise spectra for the clean airframe, the wheel-well cavities exposed, and the full landing gear deployed. The cavities were very shallow by necessity because of the very thin ($t/c=3\%$) wing. It is known that shallow cavities do not radiate intense tonal sound. Indeed, the present data show that the cavity also radiated very little broadband sound. The external landing gear was found to contribute most of the broadband noise. The noise produced a peak at 1250 Hz and added high-frequency energy to the noise spectrum. The noise could not be attributed to any single element of hardware. The landing gear was comprised of many bluff bodies (cylinders) of various shapes and sizes which experienced fluctuating forces through the shedding of their unsteady wakes. Depending upon Reynolds number, this shedding process can be either periodic or random and produces sound accordingly, either tonal or broadband. In the present tests the landing gear was coated with fine sand in an attempt to simulate the high Reynolds number, turbulent boundary layer on a full-scale aircraft. This resulted in fairly broadband radiation, as the figure indicates.

Summation of Noise Components

Contributions of the individual components above the clean airframe noise level for several directions θ in the flyover plane are presented in Table 3. As was already discussed, only the trailing-edge flaps and the landing gear were significant. The trailing-edge flap data correspond to a flap setting of 40 deg (the nominal setting for landing-approach as indicated in Table 2). The results show that flap noise is greater in the forward quadrant and less in the aft. This is consistent with the dipole description of flap noise in that the noise should be greatest in the direction normal to the flap. In contrast the main landing gear displays a uniform directivity reflecting the different orientations of the various bluff bodies comprising it. If the acoustic energy from the individual contributions made by the flaps and main gear is computed, the results added and summed with the energy from the clean airframe, and finally reconverted back to a decibel scale, a level is obtained that is several decibels above the clean airframe (see Σ components). This level would be the difference between the landing-approach configuration and the clean configuration if the component noise intensities were linearly independent. Note, however, that the measured landing-approach configuration is higher than the linear sum of the individual

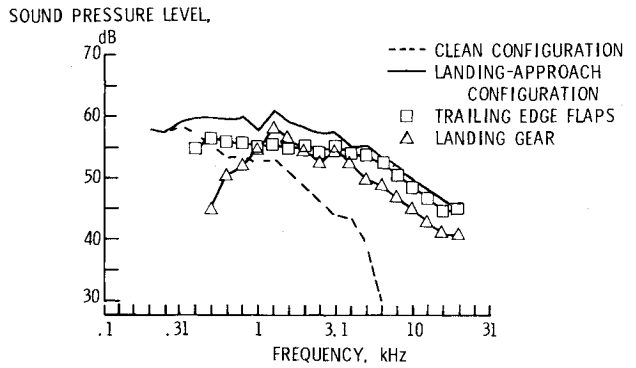

Fig. 11 One-third octave band spectra for landing-approach configuration and individual component contributions, $V = 30$ m/s, $\theta = 90$ deg, $\phi = 0$ deg.

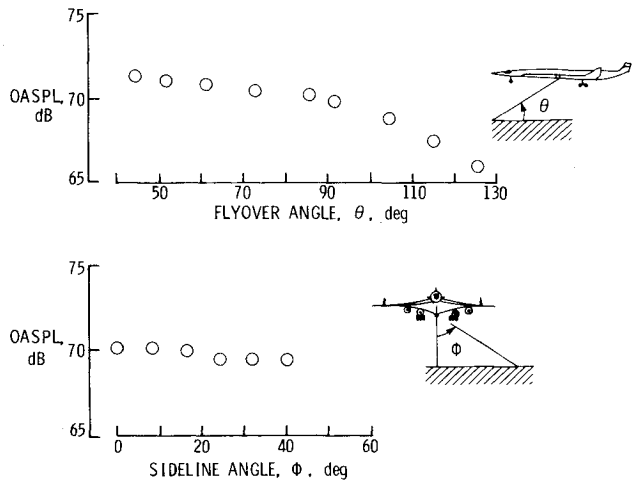

Fig. 12 Directivity pattern for landing-approach configuration, $V = 30$ m/s.

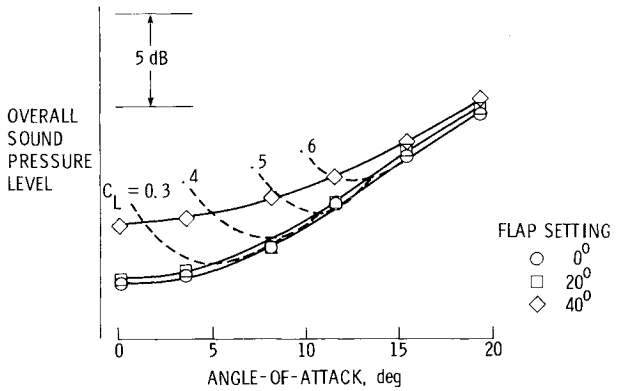

Fig. 13 Variation of overall sound pressure level with angle of attack (lines of constant lift are superimposed).

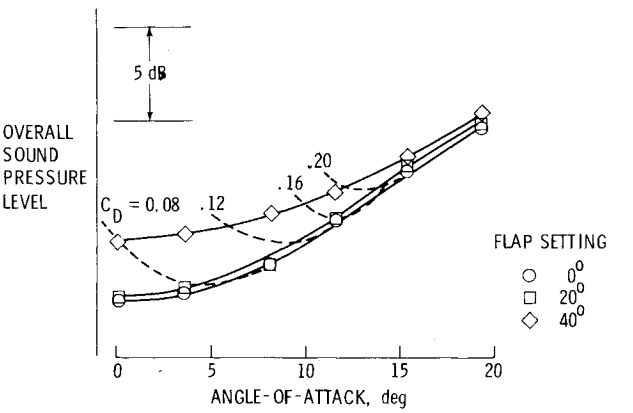

Fig. 14 Variation of overall sound pressure level with angle of attack (lines of constant drag are superimposed).

acoustic intensities. This result suggests that the components may be interacting in such a way as to increase the noise. Table 3 shows that the landing-approach configuration is noisiest in the forward quadrant. This forward quadrant also shows the largest difference between the measured noise level and the sum of the components. It is believed that an aeroacoustic interaction exists between the landing gear and trailing-edge flaps in such a way as to increase the forward-radiating flap noise. Referring to Fig. 2b, this interaction is most likely due to the highly turbulent landing-gear wake impinging on the flaps, thereby increasing the level of lift force fluctuations and, hence, the noise.

Landing-Approach Configuration

Spectra

One-third octave band spectra for the landing-approach configuration in the overhead position are presented in Fig. 11. For comparison purposes, the clean spectra and the contributions of the individual landing gear and trailing-edge flaps are also shown. As anticipated from the component spectra, the landing-approach noise is several decibels above the clean configuration with the differences becoming larger as the frequency increases. At the lowest frequencies noise radiation from the clean airframe dominates the spectra. The flaps provide a broadband contribution which has its strongest influence on the high-frequency spectra above 5000 Hz. Landing-gear noise influences the peak at 1250 Hz and also provides a high-frequency contribution.

Directivity

The directivity patterns of the landing-approach configuration in both the flyover and sideline planes are presented in Fig. 12. In contrast to the symmetric dipole configuration seen for the clean airframe in Fig. 6, the noise radiations show a large increase for shallow flyover angles and a uniform pattern at the sideline. In the flyover plane, the large increase is chiefly a result of forward-radiated noise from the deflected trailing-edge flaps, as well as a smaller contribution from the landing gear. At the sideline, it appears that no single mechanism is responsible for the high values of OASPL at large ϕ values. A difficulty in assessing the mechanisms is that the clean airframe itself does not have an experimentally well-defined sideline directivity (refer to Fig. 6). This was because the background sting noise was dipole in nature and increased with increasing ϕ values. For $\phi > 20$ deg, the clean airframe could not be "heard" over the background noise. For the landing-approach configuration useful data were obtained for values of ϕ as high as 40 deg. Component testing indicated that the landing gear (but not the wheel-well cavities), the trailing-edge flaps, and the vertical airframe surfaces (vertical tail and upper surface fins) all made some contribution to the sideline with no single element dominating. A uniform sideline directivity had been reported previously from full-scale flyover tests.[11,12]

Effect of Flaps and Angle of Attack

In Figs. 13 and 14 are presented variations of overall sound pressure level with angle of attack for several trailing-edge flap deflections. Curves of constant lift (Fig. 13) and drag (Fig. 14) for an untrimmed vehicle are superimposed on both figures. The data are for the overhead position ($\theta = 90$ deg, $\phi = 0$ deg). It is seen that for any given flap setting, the noise level increases slowly at low angles of attack and much more rapidly for larger angles. As mentioned previously, for angles of attack greater than about 6 deg, a large-scale vortex system separates from an inboard leading-edge position, rolls up, and sweeps back past the aircraft trailing edge. This vortex which

dominates the aerodynamics at large angles undoubtedly is associated with the sudden rate of change of noise production.

Note also that at a given low angle of attack there is little change in OASPL between the 0 and 20 deg flap setting but a substantial change between the 20 and 40 deg flap setting. This change is attributed to the flow separation phenomena noted previously at the high settings. Curves of constant lift in Fig. 13 suggest that during landing-approach there may be an optimum combination of flap setting and angle of attack (the "bucket" of the constant lift curves) to minimize airframe noise. Curves of constant drag in Fig. 14 show a trend similar to that for lift. A noise prediction scheme based upon aerodynamic drag has previously been suggested.[13]

Scaling

There remains, of course, the question of scaling. A 0.03 scale model of a Boeing 747 has been previously tested in an anechoic flow facility and results have been compared with full-scale measurements.[4] It was found that one-third octave band spectra agreed with ±3 dB for the case of both leading- and trailing-edge flaps deployed based upon a simple geometric scale factor relationship. However, the case for the landing gear deployed would not scale. In another study involving noise radiation from model landing gear/wheel-well combinations,[10] some agreement was obtained in scaling to full-scale results. However, more recently,[2] the same authors have stated that extreme caution must be applied in employing scaling to such a complex case as represented by landing gears, and that neither model-scale experiments nor calculations from basic principles provide the needed accuracy.

For the present tests, it was found that the clean airframe model spectra (see Fig. 5) agreed very well with a prediction method,[3] although differences in directivity and velocity dependence were observed. Because of this agreement, scaling on geometry and velocity appears to be an appropriate procedure for estimating the full-scale clean airframe spectra. If it is assumed that the mean-square acoustic pressure p^2 is proportional to V^6S/r^2, where V is the jet velocity, S is the wing area, and r is the source-observer distance, then geometric scaling need not be considered further since the microphone in the model study was placed at the appropriate scaled position for FAR-36 on approach. Using the data of Fig. 5 then, a full-scale AST-100 approaching at a speed of 87 m/s would have a clean airframe noise spectra peak of about 83 dB at a frequency of 30 Hz.

Model flap data (except for high flap settings where flow separation occurred) also followed the full-scale observation of dipole radiation normal to the flap surface. However, the magnitude of the model flap noise was seen to increase when the landing gear was deployed upstream. These component interaction effects have been observed previously in model studies,[14,15] although there is no full-scale evidence as to its importance. Hence, there is some uncertainty in how to scale this effect.

The present model data results with landing gear deployed displayed a uniform directivity which is not inconsistent with the full-scale modeling of the struts, braces, and wheels as independent bluff-body dipole radiators. However, the present vehicle was comprised of 12 wheels per landing gear. No full-scale data exists on such a configuration to compare with quantitatively. The flowfield about such a configuration must be very complex and Reynolds number effects probably play an important role.

In addition to the questions on aeroacoustic source modeling and amplitude scaling is the question of frequency scaling. Usually, to obtain a reasonable measurement of full-scale noise effects, model noise data should be considered at frequencies up to and perhaps beyond 100 kHz. But this presents difficulties from both a measurement and modeling viewpoint. If one assumes bluff-body radiation at a Strouhal number of 0.3 from some arbitrary element on the landing-approach configuration, then the 31 kHz band at model scale would correspond to a bluff body with a characteristic dimension of 1/100 in. Modeling to this fine a detail is difficult. Moreover, this characteristic dimension would be 3/4 in. on a full-scale vehicle. This degree of detail obviously has not been defined for a future supersonic transport. Hence, it is difficult to assess quantitatively what would be the effect of the high-frequency (> 31 kHz model scale) airframe noise data. Qualitatively, one would still expect the massive structures like the flaps and landing gear to generate most of the noise and, indeed, these were accurately modeled at small scale. Therefore, the high-frequency measurement limitations are not considered to be of great consequence at this time.

Conclusion

Results have been presented from airframe noise tests on a small-scale model of a supersonic transport concept in an anechoic flow facility. For the clean airframe, spectra normalization was achieved and a dipole directivity was displayed. The landing-approach configuration showed an increase in noise level over the clean configuration for all angles with the largest difference being for shallow approach angles. The increase was due chiefly to the landing gear, the trailing-edge flaps, and the interaction between the two. The airframe noise level was found to be a function of angle of attack and flap setting; noise level minimization at constant lift by proper combination of the two was indicated. Results suggested that the model clean airframe and flap data could be scaled to full scale, but some questions remain on scaling the unique 12-wheel landing gear and the component interaction effects.

References

[1] Gibson, J.S., "The Ultimate Noise Barrier – Far-field Radiated Aerodynamic Noise," *Inter-Noise 72 Proceedings*, M.J. Crocker, ed., Institute of Noise Control Engineering, 1972, pp. 332-337.

[2] Heller, H.H. and Dobrzynski, W.M., "A Comprehensive Review of Airframe Noise Research," *Proceedings of the 11th Congress of ICAS*, Lisbon, Portugal, 1978, pp. 42-60.

[3] Fink, M.R., "Noise Component Method for Airframe Noise," AIAA Paper 77-1279, Atlanta, Ga., Oct. 1977.

[4] Shearin, J.G., Fratello, D.J., Bohn, A.J., and Burggraf, W.D., "Model and Full-Scale Large Transport Airframe Noise," AIAA Paper 76-550, Palo Alto, Calif., July 1976.

[5] Coe, P.L., Jr., McLemore, H. C., and Shivers, J. P., "Effects of Upper Surface Blowing and Thrust Vectoring on Low Speed Aerodynamic Characteristics of a Large-Scale Transport Model," NASA TN D08296, 1976.

[6] Preisser, J.S., "Results from an Exploratory Study of Airframe Noise on a Small-Scale Model of a Supersonic Transport Concept," NASA TM X-74021, 1977.

[7] Amiet, R.K., "Refraction of Sound by a Shear Layer," *Journal of Sound and Vibration*, Vol. 58, 1978, pp. 467-482.

[8] Ffowcs-Williams, J.E., and Hall, L.H., "Aerodynamic Sound Generation by Turbulent Flow in the Vicinity of a Scattering Half-Plane," *Journal of Fluid Mechanics*, Vol. 40, Part 4, 1970, pp. 657-670.

[9] Coe, P.L., Jr. and Weston, R.P., "Effects of Wing Leading-Edge Deflection on the Low-Speed Aerodynamics Characteristics of a Low-Aspect Ratio Highly Swept Arrow-Wing Configuration," NASA TM 78787, 1978.

[10] Heller, H.H. and Dobrzynski, W.M., "Sound Radiation from Aircraft Wheel Well/Landing Gear Configurations," *Journal of Aircraft*, Vol. 14, Aug. 1977, pp. 768-773.

[11] Fethney, P., "An Experimental Study of Airframe Self-Noise," RAE Technical Memo AERO 1623, Feb. 1975.

[12] Lasagna, P.L. and Putnam, T.W., "Preliminary Measurements of Aircraft Aerodynamic Noise," AIAA Paper 74-572, Palo Alto, Calif., June 1974.

[13] Revell, J.D., Healy, D.J., and Gibson, J.S., "Methods for the Prediction of Airframe Aerodynamic Noise," AIAA Paper 75-539, Hampton, Va., March 1975.

[14] Shearin, J.G. and Fratello, D.J., "Airframe Noise of Component Interactions on a Large Transport Model," AIAA Paper 77-57, Los Angeles, Calif., Jan. 1977.

[15] Block, J.P.W., "An Experimental Investigation of Airframe Component Interference Noise," AIAA Paper 77-56, Los Angeles, Calif., Jan. 1977.